

# Aromatic bi-, tri- and tetracarboxylic acid doped polyaniline nanotubes: effect on morphologies and electrical transport properties†

Cite this: *J. Mater. Chem. C*, 2014, 2, 3382

Utpal Rana,<sup>a</sup> Sanjoy Mondal,<sup>a</sup> Jhuma Sannigrahi,<sup>b</sup> Pradip Kumar Sukul,<sup>a</sup> Md. Asif Amin,<sup>a</sup> Subham Majumdar<sup>b</sup> and Sudip Malik<sup>\*a</sup>

Polyaniline nanotubes have been prepared in a facile manner *via* the chemical polymerization of aniline in an aqueous medium using ammonium persulphate (APS) and ten different dopant acids. The formation of PANI in the composite was confirmed using <sup>1</sup>H-NMR, UV-Vis and FTIR spectroscopic studies. An intensive FESEM investigation indicated that the dopant acid plays an important role in the formation of the PANI nanotubes. In particular, the symmetrical positioning of –COOH groups in the aromatic dopant acid is key for forming PANI nanotubes. Symmetrical BTA-1 produces PANI nanotubes, whereas BTA-2 and BTA-3 only generate granular aggregates of PANI. The diameter of the observed nanotubes varies with the molar ratio of BTA-1 to aniline and the diameter of the nanotubes increases with the increasing number of –COOH groups in dopant acids that have the same central core. A comparative study with other tricarboxylic acids shows that the outer diameter (OD) of the PANI nanotubes depends on the size of the dopant under identical reaction conditions and follows the order: OD<sub>TPCA</sub> > OD<sub>BPCA</sub> > OD<sub>BTA-1</sub>. Low temperature charge transport in these composites mainly follows a three dimensional variable range hopping mechanism.

Received 31st October 2013  
Accepted 22nd December 2013

DOI: 10.1039/c3tc32152e

www.rsc.org/MaterialsC

## Introduction

The process of transforming a polymer into its conductive form *via* chemical oxidation or reduction is called doping.<sup>1</sup> The enhancement of electric conductivity of a polymer primarily depends on (a) the chemical reactivity of the dopant within the polymer, (b) the extent of doping and (c) the mobility of the dopant ions. The nature of the dopant plays an important role in the stability of the conducting polymer (CP).<sup>2</sup> Recent advancements in the applications of conducting polymers has fuelled research into the development of novel, as well as facile, strategies for making CPs.<sup>3</sup>

Among the different conducting polymers, polyaniline (PANI) has the greatest potential for commercial applications because of its promising properties, *e.g.*, its fast switching rate (the ability to switch reversibly from its insulating to conducting state *via* either electrochemical or chemical doping), environmental stability and processability.<sup>3</sup> Nanostructures

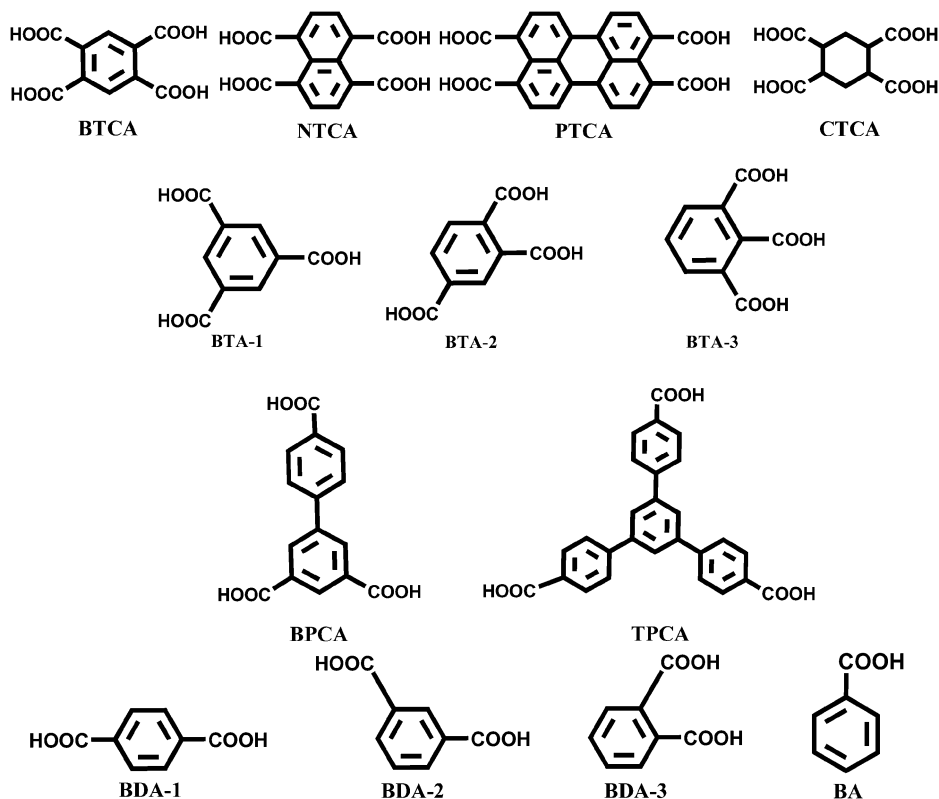
including nanorods, nanofibers, nanotubes, nanobelts *etc.* of PANI have recently received considerably more attention than bulk PANI due to their enhanced electrical properties, high conductivity and good environmental stability.<sup>4</sup> However, the synthesis of PANI nanotubes is challenging as well as painstaking. A few methods currently exist to prepare PANI nanotubes *e.g.*, hard template methods,<sup>5</sup> bio-template methods,<sup>6</sup> interfacial polymerization,<sup>7</sup> seeding,<sup>8</sup> and template-free methods that form nanotubes spontaneously in aqueous solutions.<sup>9</sup> In the hard template method, aluminium oxide and zeolites are used as templates and polymerization proceeds within the porous network of the membrane.<sup>10</sup> Tedious post-synthesis processing is often needed to remove template, damaging the PANI nanotubes. Soft template methods that employ liquid crystals, surfactants, micelles, vesicles, gels, *etc.* to synthesize PANI nanotubes, suffer from the limits of using chemicals.<sup>11</sup> Template free synthesis methods,<sup>8,12</sup> which include interfacial polymerization, nanoparticle or nanofiber seeding, electrospinning, gamma or ultraviolet irradiation, *etc.* have generated a number of potential applications for PANI nanotubes such as chemical sensors, molecular memory devices, capacitors, *etc.*<sup>13</sup>

Recently, we reported the formation of PANI nanostructures using the aromatic tetracarboxylic acids (Scheme 1) benzene-1,2,4,5-tetra carboxylic acid (BTCA), naphthalene-1,4,5,8-tetracarboxylic acid (NTCA) and perylene-3,4,9,10-tetracarboxylic acid (PTCA), which served simultaneously as both dopant

<sup>a</sup>Polymer Science Unit, Indian Association for the Cultivation of Science, 2A and 2B Raja S. C. Mullick Road, Jadavpur, Kolkata 700032, India. E-mail: psusm2@iacs.res.in

<sup>b</sup>Department of Solid State Physics, Indian Association for the Cultivation of Science, 2A and 2B Raja S. C. Mullick Road, Jadavpur, Kolkata 700032, India

† Electronic supplementary information (ESI) available: <sup>1</sup>H-NMR, <sup>13</sup>C-NMR spectra of BPCA and TPCA, as well as <sup>1</sup>H-NMR, FT-IR and UV-Vis spectra of the PANI composites. See DOI: 10.1039/c3tc32152e



Scheme 1 Chemical structures of the aromatic carboxylic acids.

acids and structure directing agents during the chemical polymerization of aniline in the presence of ammonium persulphate (APS).<sup>14</sup> The presence of these acids changes the bulk morphology of PANI from granular to nanofibers depending on the ratio of the dopant acid to aniline. It has been reported that the formation of the PANI nanotubes occurs by a self-assembly method, in which vesicles are formed from symmetrical aromatic dopant acids. These vesicles are then aggregated to form nanotubes. Meanwhile, with non-aromatic dopant acids such as cyclohexane-1,2,4,5-tetracarboxylic acid (CTCA), random aggregates are observed.<sup>15</sup> This indicates that the formation of the PANI nanotubes is possible only with tetracarboxylic acids possessing an aromatic central core that can facilitate the formation of the initial vesicular aggregates through  $\pi$ - $\pi$  interactions. Now the question is whether it is possible to make nanotubes using any type of aromatic dopant acid or whether there is any relationship between nanotube formation and the structure of the dopant.

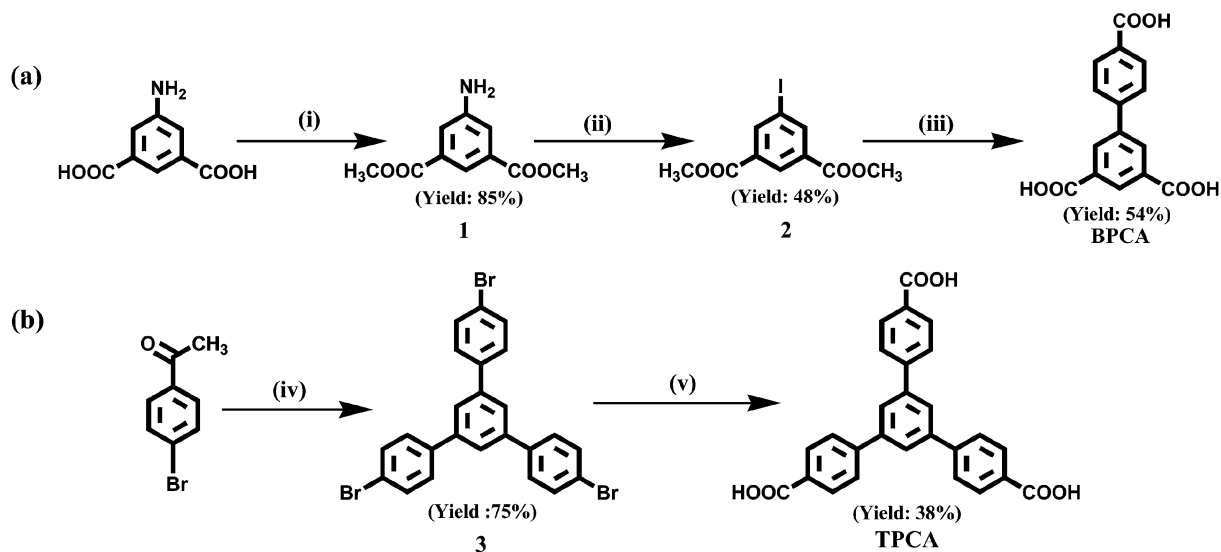
In order to address these issues, five aromatic tricarboxylic acids [1,3,5-benzene tricarboxylic (BTA-1), 1,2,4-benzene tricarboxylic (BTA-2), 1,2,3-benzene tricarboxylic (BTA-3), biphenyl-3,4',5-tricarboxylic acid (BPCA) and 1,3,5-tris(4-carboxyphenyl)benzene (TPCA)], three aromatic dicarboxylic acids [benzene-1,4-dicarboxylic acid (BDA-1), benzene-1,3-dicarboxylic acid (BDA-2), benzene-1,2-dicarboxylic acid (BDA-3)] and one aromatic monocarboxylic acid (benzoic acid) were investigated. The polymerization of aniline was carried out in a homogeneous aqueous solution of aniline, dopant acid and oxidant.

The effect of the size of the dopant acid on the overall morphology, and the conductivity have been investigated by means of proton nuclear magnetic resonance (<sup>1</sup>H-NMR) spectroscopy, UV-Vis spectroscopy, Fourier transform infrared (FTIR) spectroscopy, field emission scanning electron microscopy (FESEM), transmission electron microscopy (TEM), and conductivity measurements. Temperature dependent conductivity measurements of the samples have given us the opportunity to gain insight into the mechanism governing charge transport.

## Experimental details

### Materials

Benzoic acid (BA), benzene-1,4-dicarboxylic acid (BDA-1), benzene-1,3-dicarboxylic acid (BDA-2), benzene-1,2-dicarboxylic acid (BDA-3), benzene-1,3,5-tricarboxylic acid (BTA-1), benzene-1,2,4-tricarboxylic acid (BTA-2) and benzene-1,2,3-tricarboxylic acid (BTA-3) were purchased from Merck Chemicals. 4-Bromoacetophenone, K<sub>2</sub>S<sub>2</sub>O<sub>7</sub>, 5-amino isophthalic acid, bis(pinacolato)diboron, PdCl<sub>2</sub>(dppf) and ammonium persulphate were purchased from Sigma Aldrich. *n*-Butyl Lithium (1.6 M), KOAc, KOH, NaOH, tetrahydrofuran (THF), hydrochloric acid (HCl), sulfuric acid (H<sub>2</sub>SO<sub>4</sub>), methanol (MeOH), dry CO<sub>2</sub> and potassium iodide were purchased from local commercial sources in analytically pure grades. BPCA and TPCA were prepared in our laboratory (Scheme 2). All of the aqueous solutions were



**Scheme 2** The synthesis of (a) BPCA and (b) TPCA: (i) MeOH, H<sub>2</sub>SO<sub>4</sub>, reflux, 24 h (ii) NaNO<sub>2</sub>, dil. HCl, KI, −5 °C (iii) bis(pinacolato)diboron, methyl-4-bromobenzoate, PdCl<sub>2</sub>(dppf), KOAc, THF, NaOH, reflux (iv) H<sub>2</sub>SO<sub>4</sub>, K<sub>2</sub>S<sub>2</sub>O<sub>7</sub>, 180 °C, 16 h (v) *n*-BuLi, −60 °C, dry CO<sub>2</sub>.

prepared with 18 MΩ water obtained by purifying deionized water using a Millipore Milli-Q system.

### Instrumentation

The dopant acids and corresponding PANI composite samples were dissolved in DMSO-*d*<sub>6</sub> solvent and their <sup>1</sup>H-NMR spectra were recorded using 300 and 500 MHz Bruker NMR instruments. UV-Vis spectra of all of the PANI composites were obtained by dispersing about 0.1 mg mL<sup>−1</sup> in water then placing the samples in 1.0 cm path length cells in a Hewlett-Packard UV-Vis spectrophotometer (model 8453). FTIR spectra were scanned from 400–4000 cm<sup>−1</sup> with an FTIR-8400S instrument (Shimadzu) using KBr pellets of the samples. In order to observe the surface morphology, a tiny amount of each sample was dispersed in Milli Q water then drop cast onto a glass cover slip at room temperature before investigation. For the FESEM observations, a JSM 6700F (JEOL) microscope operating at 5 kV was used. The samples were coated with platinum over 80 s in order to reduce the surface potential due to the accumulation of electrostatic charge. The HRTEM investigations were carried out by spreading each sample onto a Cu-grid coated with a holey carbon support film and micrographs were taken at an accelerating voltage of 200 kV using a JEOL, 2010EX microscope equipped with a CCD camera. The temperature (*T*) dependent electrical resistivity of the samples was measured using a four point method with a Keithley nanovoltmeter (model 2182A) and constant current source (model 2400) in a nitrogen cryostat between 77 and 300 K. The optimum current used for the measurement was 10 μA. The samples were pelletized and connections were made using silver epoxy.

### Preparation of BPCA

**Synthesis of 5-aminobenzene-1,3-dicarboxylate (1).** 5-Amino isophthalic acid (5.0 g, 27.6 mmol) was dissolved in methanol

(150 mL). Concentrated H<sub>2</sub>SO<sub>4</sub> (3 mL) was then added and the solution was refluxed overnight. The solvent was removed using a rotary evaporator and the residue was dissolved in chloroform (250 mL), washed with saturated bicarbonate and the solvent was removed again under reduced pressure to give 4.9 g of the desired product **1** as a white powder (Yield: 85%). <sup>1</sup>H-NMR (300 MHz, CDCl<sub>3</sub>): δ 3.90 (s, 6H), 7.51 (s, 2H), 8.04 (s, 1H) ppm. <sup>13</sup>C NMR (300 MHz, CDCl<sub>3</sub>): δ 52.4, 119.8, 120.7, 131.6, 146.8, 166.6 ppm. HRMS: calcd for C<sub>10</sub>H<sub>11</sub>NO<sub>4</sub> 209.20, found 210.01 (MH<sup>+</sup>), 231.9 (MNa<sup>+</sup>).

**Dimethyl 5-iodobenzene-1,3-dicarboxylate (2).** A solution of sodium nitrite (15 g, 0.21 mol) in water (200 mL) was added to a suspension of 5-aminobenzene-1,3-dicarboxylate (**1**) (43.75 g, 0.21 mol) in 20% HCl (100 mL) at −5 °C. Toluene (250 mL) and then a solution of potassium iodide (70.56 g, 0.84 mol) in water (150 mL) were slowly added to the suspension. After the addition, the reaction mixture was stirred for 16 h and then refluxed for 2 h. The organic layer was separated and washed several times with water, then dried with NaSO<sub>4</sub>, filtered, and concentrated under vacuum. The crude product was purified by column chromatography (silica gel, ethyl acetate/hexane, 3 : 7 v/v) and recrystallized from methanol, giving 7.94 g of **2** as light-brown crystals (Yield: 48%). <sup>1</sup>H-NMR (300 MHz, CDCl<sub>3</sub>): δ = 3.95 (s, 6H), 8.53 (d, 2H), 8.61 (t, 1H) ppm. <sup>13</sup>C NMR (300 MHz, CDCl<sub>3</sub>): δ = 52.6, 93.4, 129.8, 132.3, 142.4, 164.7 ppm.

**Biphenyl-3,4',5-tricarboxylic acid (BPCA).** A mixture of dimethyl 5-iodobenzene-1,3-dicarboxylate (**2**) (500 mg, 1.56 mmol), bis(pinacolato)diboron (360 mg, 1.41 mmol), potassium acetate (460 mg, 3.00 mmol), PdCl<sub>2</sub>(dppf) (40 mg, 0.05 mmol), and dried DMF (15 mL) was stirred at 80 °C for 2 h. The reaction mixture was cooled to room temperature. Methyl 4-bromobenzoate (990 mg, 3.20 mmol), PdCl<sub>2</sub>(dppf) (40 mg, 0.05 mmol), and KF (760 mg, 5.0 mmol, dissolved in 3.5 mL of water) were then added. The mixture was stirred at 80 °C overnight and then

extracted several times with diethyl ether. The organic layer was dried with  $\text{NaSO}_4$ , and the solvent was removed under vacuum. The crude product was purified by column chromatography (silica gel, ethyl acetate/hexane, 3 : 7 v/v). Subsequently, it was hydrolysed as follows: a mixture of biphenyl-3,4',5-methyltricarboxylate (1.15 g, 3.00 mmol), THF (45 mL) and NaOH (1.6 g, 40 mmol) dissolved in water (50 mL) was refluxed for 2 h. The organic solvent was then removed under reduced pressure, and the aqueous solution was refluxed again for 4 h. The reaction mixture was cooled and acidified with 50%  $\text{H}_2\text{SO}_4$ . The precipitate was filtered and dried to obtain 240 mg of BCPA as a white powder (Yield 54%).  $^1\text{H-NMR}$  (300 MHz,  $\text{DMSO-d}_6$ ):  $\delta$  = 7.86–7.87 (d, 2H), 8.04–8.06 (d, 2H), 8.41 (s, 1H), 8.48 (s, 1H), 13.28 (s, 3H) ppm.  $^{13}\text{C NMR}$  (300 MHz,  $\text{DMSO-d}_6$ ):  $\delta$  = 127.1, 129.47, 130.4, 131.4, 132.2, 140, 142.4, 166.3, 167 ppm. MS (MALDI-TOF) calcd 286.05 found 309.1  $[\text{M}^+\text{Na}]^+$ . FTIR: 3258, 1737, 1696, 1609, 1451, 1392, 1281  $\text{cm}^{-1}$ .

### Preparation of TPCA

**Synthesis of 1,3,5-tri(4-bromophenyl)benzene (3).** A mixture of 4-Bromoacetophenone (15 g, 75.37 mmol), 1.0 mL of  $\text{H}_2\text{SO}_4$  (conc.) and  $\text{K}_2\text{S}_2\text{O}_7$  (20 g, 78.67 mmol) was heated at 180 °C for 16 h under a nitrogen atmosphere. The resulting crude solid was cooled to room temperature and refluxed in 100 mL of dry EtOH for 2 h and then cooled to room temperature. The solution was filtered and the resulting solid was refluxed in 100 mL of  $\text{H}_2\text{O}$  to yield a pale-yellow solid that was then filtered. The crude product was dried under vacuum affording 30.6 g of dried product, which was recrystallized from  $\text{CHCl}_3$  (Yield : 75%).  $^1\text{H-NMR}$  (300 MHz,  $\text{CDCl}_3$ ):  $\delta$  = 7.53 (d, 6H), 7.60 (d, 6H), 7.68 (s, 3H) ppm.  $^{13}\text{C NMR}$  (300 MHz,  $\text{CDCl}_3$ ):  $\delta$  = 122.2, 125.1, 129, 132.2, 139.7, 141.6 ppm.

**Synthesis of 1,3,5-tris(4-carboxyphenyl)benzene (TPCA).** 1,3,5-Tri(4-bromophenyl)-benzene (5 g, 9.2 mmol) was dissolved in 50 mL of anhydrous THF under a  $\text{N}_2$  atmosphere. The stirred solution was cooled to –60 °C and a 1.6 M solution of *n*-BuLi in hexanes (14 mL, 18.62 mmol) was added dropwise. A red to light-green precipitation of the aryl lithium derivative was formed. Pre-dried gaseous carbon dioxide was passed into the mixture at –60 °C resulting in a colourless precipitate of the lithium salt. The mixture was allowed to warm and then was quenched with 50% aqueous acetic acid. The solid product was filtered and recrystallized from acetic acid to give 1.53 g (38%) of TPCA as white microcrystals.  $^1\text{H-NMR}$  ( $\text{DMSO-d}_6$ ):  $\delta$  = 8.06 (s, 12H), 8.09 (s, 3H) ppm,  $^{13}\text{C NMR}$  (300 MHz,  $\text{DMSO-d}_6$ ):  $\delta$  = 125.6, 127.4, 129.9, 130.0, 140.8, 143.8, 167.2 ppm. HRMS calcd 438.1 found 439.2  $[\text{M}^+\text{H}]^+$ . FTIR: 3072, 2984, 1689, 1611, 1421, 1317, 1291, 1244  $\text{cm}^{-1}$ .

**Preparation of polyaniline nanostructure.** PANI composites were synthesized by dispersing aniline (102 mg, 1.1 mmol) and the required amount of dopant acid (0.26 mmol) in water, under constant stirring for 1 h. After cooling the mixture to 10 °C, an aqueous solution of ammonium persulphate  $[(\text{NH}_4)_2\text{S}_2\text{O}_8]$ , APS, 250 mg, 1.1 mmol was added over 30 min and the mixture was allowed to stand for 24 h at low temperature. The resultant precipitate was filtered and washed ten times with water and

methanol to remove APS and oligoaniline. Finally, the precipitate was dried under vacuum overnight to afford the corresponding PANI composite.<sup>14,15</sup>

## Results and discussion

The polymerization reaction is generally carried out in a homogeneous aqueous solution of aniline, dopant acid, and APS (Table S1†). After washing several times with water and drying, the resulting PANI composites were studied by  $^1\text{H-NMR}$ , FT-IR and UV-Vis spectroscopy in order to determine the formation of polyaniline using these aromatic acids. The  $^1\text{H-NMR}$  spectra of all of the PANI nanocomposites show the three well known –NH proton resonance triplet peaks of PANI including the characteristics peaks of dopant acids. The splitting of the peaks at 6.98–7.2 ppm can be assigned to the aromatic H-resonance of the PANI chains. The presence of three sharp 1/1/1 triplets with almost equal intensity at ~6.98, 7.08, and 7.18 ppm with a coupling constant of 51.1 Hz is due to the free radical –NH proton resonance, which proves the formation of PANI (Fig. S5†).<sup>15,16</sup>

FT-IR spectra of all of the PANI composites exhibit stretching bands at ~1576, ~1483, ~1293, ~1109 and ~792  $\text{cm}^{-1}$  (Fig. S6†). The characteristic stretching vibrations at ~1576  $\text{cm}^{-1}$  ( $\gamma\text{C}=\text{C}$  for quinoid rings), ~1483  $\text{cm}^{-1}$  ( $\gamma\text{C}=\text{C}$  for benzenoid rings), ~1293  $\text{cm}^{-1}$  ( $\gamma\text{C}-\text{N}$  for the secondary aromatic amine), 1109 and 792  $\text{cm}^{-1}$  ( $\gamma\text{C}-\text{H}$  aromatic in plane and the out of plane deformation for the 1,4-disubstituted benzene) are the characteristics bands of the emeraldine salt form of PANI.<sup>17</sup>

UV-Vis spectra of all of the PANI composites show characteristic absorption peaks centered ~360, ~450 and ~925 nm (Fig. S7†). The peak at ~360 nm can be assigned to the  $\pi-\pi^*$  transition of the benzenoid rings, peak at ~450 nm can be attributed to the polaron- $\pi^*$  transition and finally the peak ~925 nm is due to the  $\pi$ -polaron transition in PANI. The presence of these three peaks indicates that the PANI chains are in an emeraldine salt state. In case of BTA-1/PANI at different molar concentrations the peak intensity at ~450 nm and ~925 nm increases with the increasing ratio from 0.01 to 0.25 because there will be more charged polarons in the PANI chains in case of the 0.25 ratio and less in the 0.01 ratio.<sup>18</sup>

### Morphological studies

FESEM images of isomeric acid doped PANI are shown Fig. 1. BTA-1, BTA-2 and BTA-3 have the same number of functional groups. BTA-1 contains three –COOH groups in symmetrical positions, but the other two contain three –COOH groups situated in asymmetric positions. It has been found that only BTA-1 produces the nanofibers, however, BTA-2 and BTA-3 produce a granular morphology. The same trend is also observed in the case of the benzene dicarboxylic acids (Fig. S8†). The formation of nanofibers using BTA-1/BDA-1 is possible because of the symmetrical positions of the –COOH groups in the dopant structure. Therefore, BTA-1 or BDA-1 can interact with aniline to





Fig. 1 FESEM-images of (a) BTA-1/PANI, (b) BTA-2/PANI and (c) BTA-3/PANI. Synthesis conditions: [acid]/[aniline] = 0.25, [aniline]/[APS] = 1.00.

form aniline filled BTA-1 or BDA-1 vesicles which self-assemble one dimensionally to form nanofibers or nanotubes. Although PANI is produced using asymmetric dopant acids, the irregular arrangement of the  $\text{-COOH}$  groups in these dopants restricts the formation of a regular structure of PANI. Thus, an aromatic dopant with  $\text{-COOH}$  groups in symmetrical positions is a key parameter for PANI nanofiber formation.

Now the next question is whether all of the aromatic acids that contain symmetrical  $\text{-COOH}$  groups are able to form vesicles. In order to address this issue, benzene 1,4-dicarboxylic acid (BDA-1) with  $C_2$ -symmetry, benzene 1,3,5-tricarboxylic acid (BTA-1) with  $C_3$ -symmetry and benzene 1,2,4,5-tetracarboxylic acid (BTCA) with  $C_{2v}$ -symmetry were chosen to investigate the PANI nanotube formation mechanism. These three acids have different numbers of  $\text{-COOH}$  groups, which are present at symmetrical positions on the aromatic core. Surprisingly, all three of the symmetric aromatic acids produce micro-meter sized nanotubes with high aspect ratios ( $\sim 55$  for BDA-1/PANI,  $\sim 65$  for BTA-1/PANI and  $\sim 300$  for BTCA/PANI). The surface smoothness of the nanotubes decreases from BDA-1/PANI to BTCA/PANI. The BDA-1/PANI nanotubes have a very rough surface because of the limited solubility of BDA-1 in water (Fig. 2).<sup>19</sup> The corresponding HRTEM images show the distinct contrast between the core and edge of the nanofibers, proving the formation of the PANI nanotubes.

In addition, the diameter of the nanotubes increases with the increasing number of  $\text{-COOH}$  groups in the dopant. The diameter for BDA-1/PANI is 148 nm, BTA-1/PANI is 156 nm and for BTCA/PANI it is 164 nm.<sup>20</sup> The diameter of the nanofibers is also controlled by changing the BTA-1/aniline ratio. The average diameter was increased from 144 nm to 156 nm upon increasing the ratio of BTA-1/aniline from 0.01 to 0.25 (Fig. 3). These changes might result from the fact that the environment for the self-assembly process is slightly different at the various concentrations of dopant acid and aniline monomer.<sup>21</sup>

It is well known that the properties of PANI (ES) is solely dependant on the nature of the dopant acids. The inter chain distance of PANI can be easily modified by using different sizes of dopant.<sup>22</sup> In addition, the size of the dopant has an influence on the delocalization of polarons through the PANI

chains in 3D regions and it plays a significant role in inducing the electrical properties of PANI.<sup>23</sup> BTA-1, biphenyl 3,5,4'-tricarboxylic acid (BPCA) and 1,3,5-tris(4-carboxyphenyl)-benzene (TPCA) are dopant acids of different sizes and were used for PANI synthesis. All of these dopant acids contain the same number of functional groups in symmetrical positions, but have different size central aromatic cores. All of the acids yield fibrillar PANI after using a 'soft-template' method under identical reaction conditions. The average diameter of the nanofibers increases from 156 nm to 166 nm with increasing core size of the dopant from BTA-1 to TPCA, as shown in Fig. 4. The increase of diameter of the nanofibers with increasing size of the dopant is possibly due to the formation of larger vesicles for TPCA in the early stages of the reaction due to molecular aggregation of the dopant acid with aniline monomer.<sup>21</sup>

### Transport studies

The thermal variation of the electrical resistivity ( $\rho$ ) for the samples studied is shown in Fig. 5, where  $\ln \rho$  is plotted against  $T^{0.25}$ . It should be noted that in the case of three dimensional (3D) variable range hopping (VRH) conduction, one would expect  $\ln(\rho/\rho_0) = (T_0/T)^{0.25}$ , where  $T_0$  is the characteristic temperature associated with the hopping mechanism, and  $\rho_0$  is a constant. VRH conduction is often observed in disordered solids, where the hopping of charge carriers is not necessarily restricted among their nearest neighbor sites. All of the curves [except BPCA (0.25)] are found to be linear in the measured temperature window indicating 3D VRH type conduction. Such a type of electrical conduction has been reported in other acid doped PANI samples.<sup>24</sup> This can be attributed to the fact that the charge carriers generated from the protonation of PANI move in a spatially random potential, leading to VRH conduction. Notably, for BPCA (0.25) (Fig. 5(a)), a shoulder like feature is observed around  $1/T^{0.25} = 0.28$  ( $T \sim 160$  K). The origin of this feature not clear at the moment. We have only used low- $T$  data for this particular sample for analysis. In these PANI chain systems, one might expect to observe quasi one dimensional conduction. However the predominant 3D character can often be attributed to the extension of the electronic wave function over the polymer bundle.<sup>25</sup> In order to gain more insight into the

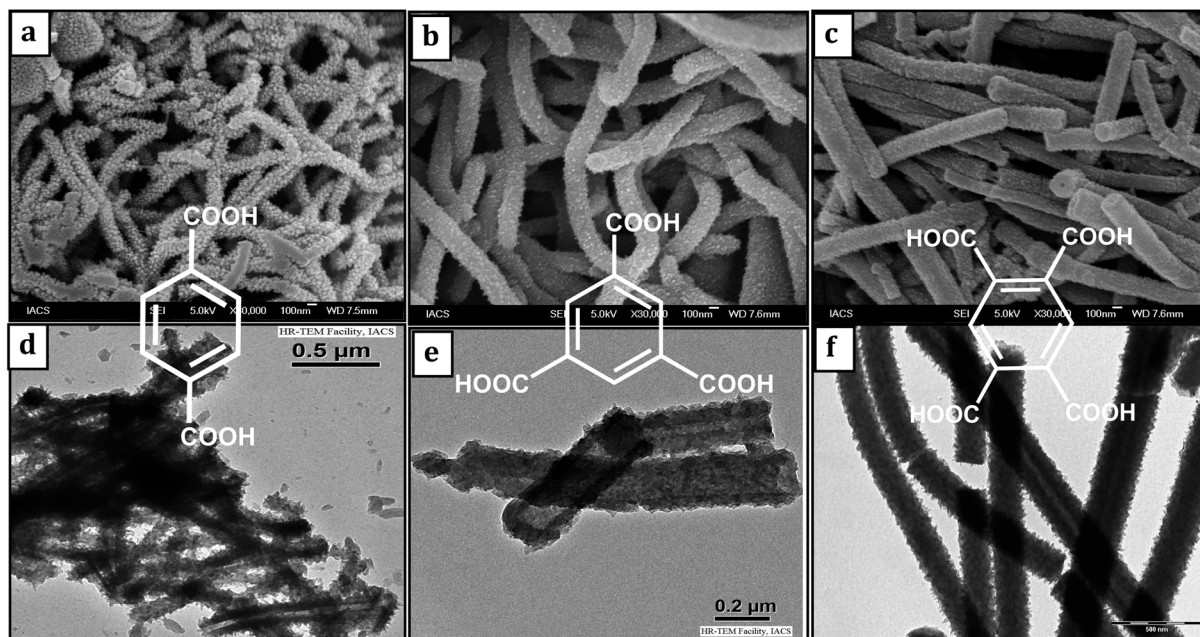


Fig. 2 FESEM images PANI nanofibers doped by different aromatic carboxylic acids, (a) BDA-1/PANI, (b) BTA-1/PANI, (c) BTCA/PANI and their corresponding HRTEM images in (d), (e) and (f). Synthesis condition, [acid]/[aniline] = 0.25, [aniline]/[APS] = 1.

conduction mechanism in the samples, we have performed a least square fitting of the data using the above equation and the solid lines in Fig. 5 represent the fitted curves. The fitted values of  $T_0$  and the room temperature conductivity ( $\sigma = 1/\rho$ ) have been tabulated in Table S2.† It should be noted that  $\sigma$  is found to range between  $0.5 \times 10^{-3}$ – $58.8 \times 10^{-2}$  S cm $^{-1}$ . The room temperature bulk conductivity of the PANI nanotubes is

relatively low compared with PANI composites doped with inorganic acids and this is possibly due to the lower mobility of the organic dopants. The highest room temperature conductivity is observed for BPTA, which is presumably related to the ordered arrangements of the polymer chains (Fig. 4c and d). The value of  $T_0$  is found to be in the order of  $\sim 10^7$  K, which is similar to that found for H $_3$ PO $_4$ -doped polyaniline.<sup>24</sup>

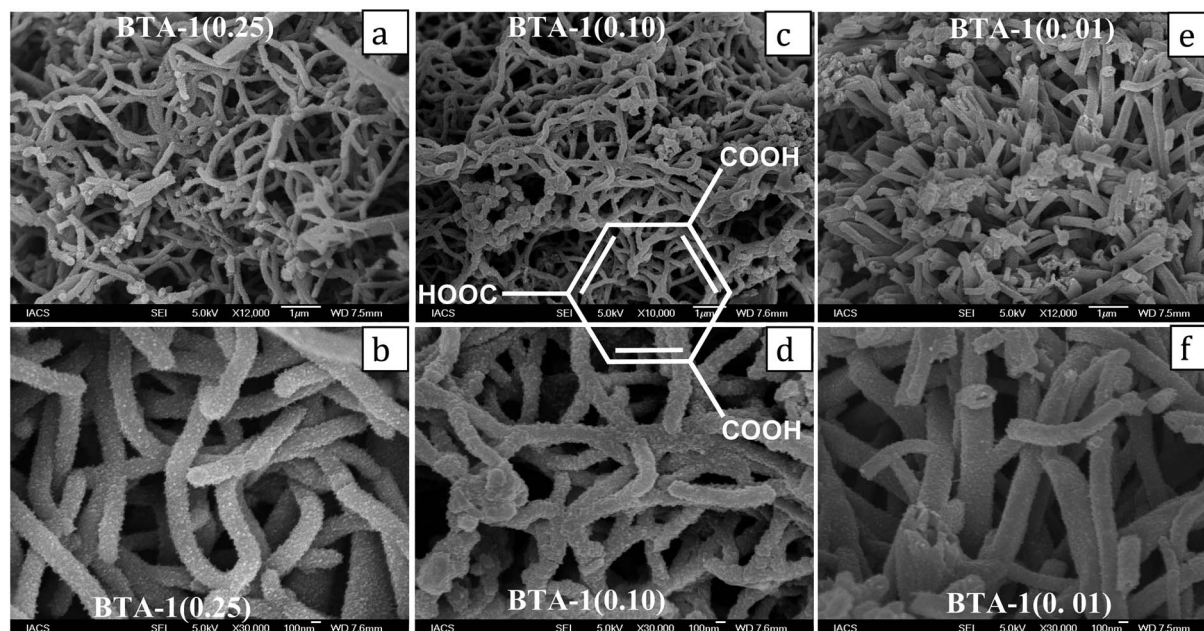


Fig. 3 Low and high magnification FESEM images of three different molar ratios of BTA-1 to aniline: (a and b) 0.25, (c and d) 0.10 and (d and e) 0.01. [aniline]/[APS] = 1.00.



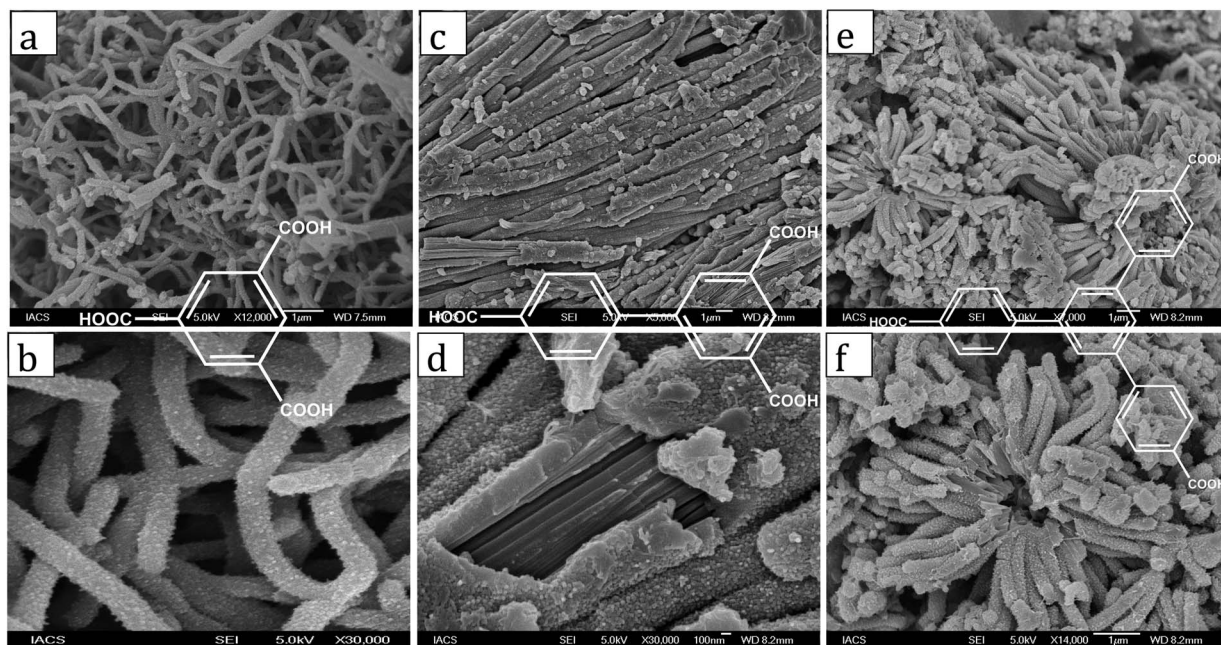


Fig. 4 Low and high magnification FESEM images of different tricarboxylic acid-PANI samples: (a and b) BTA-1/PANI, (c and d) BPCA/PANI and (e and f) TPCA/PANI. [acid]/[aniline] = 0.25, [aniline]/[APS] = 1.00.

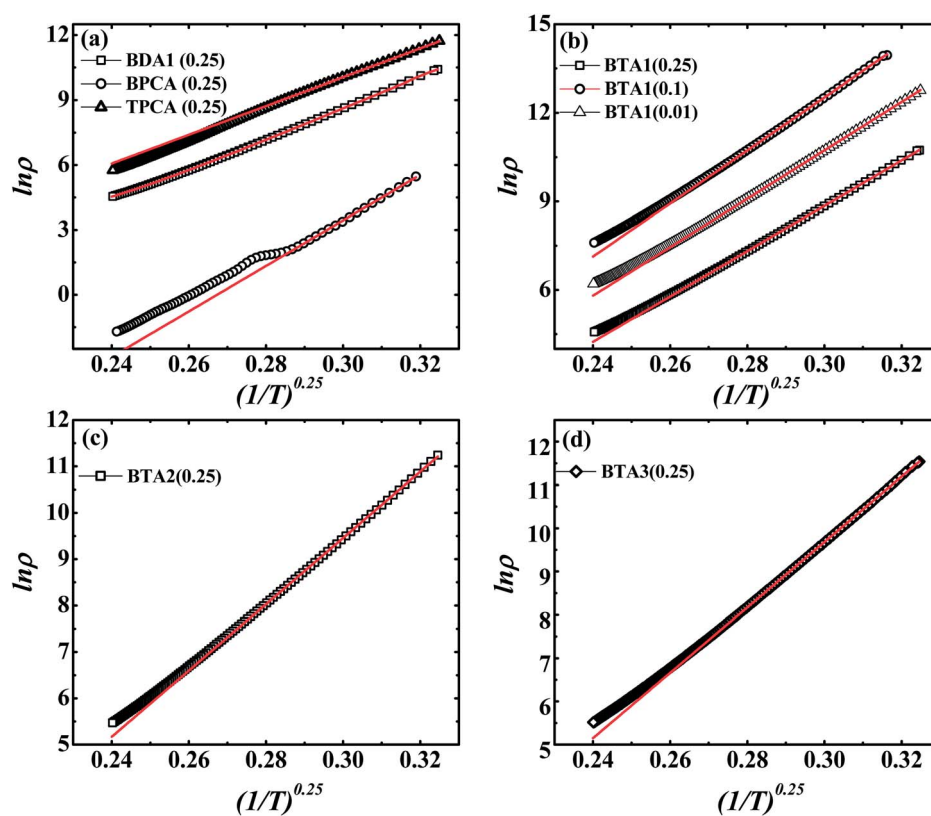


Fig. 5 Thermal variation of the dc resistivity (in Ohm cm) scaled to the variable range hopping model (VRH) for the various samples. The solid straight red lines indicate the fitted curves (see text for details).

## Conclusion

Using ten different aromatic acids, PANI nanotubes have been prepared *via* the chemical polymerization of aniline. An intensive morphological investigation indicates that the structure of the dopant acid as well as the symmetrical positioning of its functional groups plays a critical role in the formation of the PANI nanotubes. The diameter of the PANI nanotubes varies with the molar ratio of the dopant acid to aniline, the number of functional groups present in dopants with the same central core and also the size of the central core in dopants that have the same number of functional groups. The conductivity of the composites are in the range of  $0.58 \times 10^{-3}$ – $58.8 \times 10^{-2}$  S cm<sup>-1</sup> and three dimensional variable range hopping (VRH) type conduction was observed for all of the aromatic acid doped PANI samples. The present method provides a facile template-free method towards PANI nanotubes, which can be used for plastic based nanoelectronics applications.

## Acknowledgements

S. M. and P. K. S. are indebted to CSIR, New Delhi, India for financial support. Md. A. A. is indebted to the Department of Science and Technology (DST), Govt. of India, for providing an INSPIRE fellowship (Reg. no. 381/2009). The authors are thankful to the Unit of Nanoscience (DST, Govt. of India) at IACS.

## References

- 1 A. G. MacDiarmid, *Angew. Chem., Int. Ed.*, 2001, **40**, 2581.
- 2 (a) A. A. Syed and M. K. Dinesan, *Talanta*, 1991, **38**, 815; (b) H. D. Tran, J. M. D'Arcy, Y. Wang, P. J. Beltramo, V. A. Strong and R. B. Kaner, *J. Mater. Chem.*, 2011, **21**, 3534.
- 3 (a) M. Wan, *Macromol. Rapid Commun.*, 2009, **30**, 963; (b) P. Liu and L. Zhang, *Crit. Rev. Solid State Mat. Sci.*, 2009, **34**, 75; (c) A. Eftekhari, *Nano-structured Conductive Polymers*, Wiley, London, UK, 2010, p. 19; (d) J. Stejskal, I. Sapurina and M. Trchova, *Prog. Polym. Sci.*, 2010, **35**, 1420; (e) C. Laslau, Z. Zucovic and J. Travas-Sejdic, *Prog. Polym. Sci.*, 2010, **35**, 1403; (f) H. D. Tran, J. M. D'Arcy, Y. Wang, P. J. Beltramo, V. A. Stron and R. B. Kaner, *J. Mater. Chem.*, 2011, **21**, 3534; (g) G. Ciric-Marjanovic, *Synth. Met.*, 2013, **177**, 1; (h) J. Wang and D. Zhang, *Adv. Polym. Technol.*, 2013, **32**, E323; (i) D. Li, J. Huang and R. B. Kaner, *Acc. Chem. Res.*, 2009, **42**, 135.
- 4 G. Li and Z. Zhang, *Macromolecules*, 2004, **37**, 2683.
- 5 (a) L. J. Pan, L. Pu, Y. Shi, S. Y. Song, Z. Xu, R. Zhang and Y. D. Zheng, *Adv. Mater.*, 2007, **19**, 461; (b) V. M. Cepak and C. R. Martin, *Chem. Mater.*, 1999, **11**, 1363.
- 6 Z. W. Niu, M. Bruckman, V. S. Kotakadi, J. B. He, T. Emrick, T. P. Russell, L. Yang and Q. Wang, *Chem. Commun.*, 2006, 3019.
- 7 J. Huang and R. B. Kaner, *Angew. Chem., Int. Ed.*, 2004, **43**, 5817.
- 8 X. Zhang, W. J. Goux and S. K. Manohar, *J. Am. Chem. Soc.*, 2004, **126**, 4502.
- 9 (a) M. Wan, *Adv. Mater.*, 2008, **20**, 2926; (b) H. Ding, J. Shen, M. Wan and Z. Chen, *Macromol. Chem. Phys.*, 2008, **209**, 864.
- 10 (a) C. G. Wu and T. Bein, *Science*, 1994, **264**, 1757; (b) C. Wang, Z. Wang, M. Li and H. Li, *Chem. Phys. Lett.*, 2001, **341**, 431.
- 11 (a) K. Huang and M. Wan, *Chem. Mater.*, 2002, **14**, 3486; (b) J. Han, G. Song and R. Guo, *J. Polym. Sci., Part A: Polym. Chem.*, 2006, **44**, 4229; (c) X. Zhang and S. K. Manohar, *Chem. Commun.*, 2004, 2360.
- 12 (a) H. X. He, C. Z. Li and N. J. Tao, *Appl. Phys. Lett.*, 2001, **78**, 811; (b) A. G. MacDiarmid, W. E. Jones Jr, I. D. Norris, J. Gao, A. T. Johnson Jr, N. J. Pinto, J. Hone, B. Han, F. K. Ko, H. Okuzaki and M. Llaguno, *Synth. Met.*, 2001, **119**, 27; (c) J. Huang and R. B. Kaner, *J. Am. Chem. Soc.*, 2004, **126**, 851; (d) R. W. Cumberland, M. B. Weinberger, J. J. Gilman, S. M. Clark, S. H. Tolbert and R. B. Kaner, *J. Am. Chem. Soc.*, 2005, **127**, 7264; (e) N. R. Chiou and A. J. Epstein, *Adv. Mater.*, 2005, **17**, 1679; (f) X. Jing, Y. Wang, D. Wu, L. She and Y. Guo, *J. Polym. Sci., Part A: Polym. Chem.*, 2006, **44**, 1014; (g) X. Lu, H. Mao, D. Chao, W. Zhang and Y. Wei, *Macromol. Chem. Phys.*, 2006, **207**, 2142.
- 13 H. D. Tran, I. Norris, J. M. D'Arcy, H. Tsang, Y. Wang, B. R. Mattes and R. B. Kaner, *Macromolecules*, 2008, **41**, 7405.
- 14 (a) U. Rana, K. Chakrabarti and S. Malik, *J. Mater. Chem.*, 2011, **21**, 11098; (b) P. Pretov, P. Mokreva, C. B. Tsvetanov and L. Terlemezyan, *Colloid Polym. Sci.*, 2008, **268**, 691; (c) L. Zhang and M. Wan, *Adv. Funct. Mater.*, 2003, **13**, 815.
- 15 U. Rana, K. Chakrabarti and S. Malik, *J. Mater. Chem.*, 2012, **22**, 15665.
- 16 (a) S. Mu and Y. Yang, *J. Phys. Chem. B*, 2008, **112**, 11558; (b) X. Wang, T. Sun, C. Wang, C. Wang, W. Zhang and Y. Wei, *Macromol. Chem. Phys.*, 2010, **211**, 1814.
- 17 (a) B. A. Deore, I. Yu and M. S. Freund, *J. Am. Chem. Soc.*, 2004, **126**, 52; (b) U. Rana and S. Malik, *Chem. Commun.*, 2012, **48**, 10862.
- 18 (a) X. G. Li, A. Li and M. R. Huang, *Chem.-Eur. J.*, 2008, **14**, 10309; (b) S. Bhattacharya, U. Rana and S. Malik, *J. Phys. Chem. C*, 2013, **117**, 22029.
- 19 Z. Zhang, Z. Wei, L. Zhang and M. Wan, *Acta Mater.*, 2005, **53**, 1373.
- 20 L. Zhang, Y. Long, Z. Chen and M. Wan, *Adv. Funct. Mater.*, 2004, **14**, 693.
- 21 Z. Zhang, M. Wan and Y. Wei, *Adv. Funct. Mater.*, 2006, **16**, 1100.
- 22 A. Kobayashi, X. F. Xu and H. Ishikawa, *J. Appl. Phys.*, 1992, **72**, 5702.
- 23 (a) Y. F. Lin, C. H. Chen, W. J. Xie, S. H. Yang, C. S. Hsu, M. T. Lin and W. B. Jian, *ACS Nano*, 2011, **5**, 1541; (b) Y. Longa, Z. Chena, N. Wang, Z. Zhang and M. Wan, *Physica B*, 2003, **325**, 208.
- 24 J. F. Rouleau, J. Goyette, T. K. Bose, R. Singh and R. P. Tandon, *Phys. Rev. B: Condens. Matter Mater. Phys.*, 1995, **52**, 4801.
- 25 Z. H. Wang, E. M. Scherr, A. G. MacDiarmid and A. J. Epstein, *Phys. Rev. B: Condens. Matter Mater. Phys.*, 1992, **45**, 4190.